Torque Ripple Minimization in Switched Reluctance Motor Using Passivity-Based Robust Adaptive Control

M.M. Namazi, S.M. Saghaiannejad, and A. Rashidi

***Abstract*—**In this paper by using the port-controlled Hamiltonian (PCH) systems theory, a full-order nonlinear controlled model is first developed. Then a nonlinear passivity-based robust adaptive control (PBRAC) of switched reluctance motor in the presence of external disturbances for the purpose of torque ripple reduction and characteristic improvement is presented. The proposed controller design is separated into the inner loop and the outer loop controller. In the inner loop, passivity-based control is employed by using energy shaping techniques to produce the proper switching function. The outer loop control is employed by robust adaptive controller to determine the appropriate Torque command. It can also overcome the inherent nonlinear characteristics of the system and make the whole system robust to uncertainties and bounded disturbances. A 4KW 8/6 SRM with experimental characteristics that takes magnetic saturation into account is modeled, simulation results show that the proposed scheme has good performance and practical application prospects.

***Keywords*—**Switched Reluctance Motor, Port Hamiltonian System, Passivity-Based Control, Torque Ripple Minimization

I. Introduction

In recent years, there is a growing concern about the use of switched reluctance motor. The major reasons for SRM are robustness, high efficiency, low cost, high speed, simple structure, easy to maintain, high controllability, high torque to inertia ratio, simple power converter circuits with reduced number of switches and smaller dimension of the motor in comparison to the other motors. High torque ripple and acoustic noise are most disadvantages of the motor. Main reason of these problems is the stepping nature and inherent nonlinear characteristics of the motor, which causes an undesired effect on bearing. If the problems of the SRM can be solved, it can be an alternative to the other motors [1].

M.M. Namazi is with the Department of Electrical and Computer Engineering, Isfahan University of Technology, Isfahan, Iran (e-mail: mm.namaziesfahani@ ec.iut.ac.ir).

S.M. Saghaiannejad, is with the Department of Electrical and Computer Engineering, Isfahan University of Technology, Isfahan, Iran (e-mail: saghaian@cc.iut.ac.ir).

A. Rashidi is with the Department of Electrical and Computer Engineering, Isfahan University of Technology, Isfahan, Iran (e-mail: 315.amir@gmail.com).

The nonlinear characteristics include the nonlinear torque function of position and current and the magnetic saturation at certain operation regions. There are two approaches followed for torque ripple minimization. One is improve the magnetic design of the motor while the other is use of advanced control techniques. Several control methods and schemes have been proposed to overcome these problems. For example, variable structure controller made the SRM drive system insensitive to parameter variations and load disturbance [2]. Artificial neural network and fuzzy controller needs a lot of designer experience [3]. Feedback linearization controller has high sensitivity to model uncertainties [4]. Nonlinear internal model control for SRM drive required very complicated computations and implementation of the system is very difficult [5].

In the methods mentioned above, for the control strategies of the SRM it is assumed that its parameters are known exactly or the unknown parameters can be identified by the adaptive technique. However the parameters of the SRM are not exactly known and always vary with current and position. Actually, control is difficult to implement owing to its complex algorithm when considering the structural information of SRM in design. Improving the applicability of the SRM on the basis of the simplified model and taking the structural characteristics into account is a significant step in designing the controller of the SRM.

In this paper, a nonlinear feedback controller, which effectively use the natural energy dissipation properties of the SRM is proposed. Passivity–based Control (PBC), introduced in [6], to define a controller design methodology which achieves stabilization by passivation [7].

Paper is organized as follows. At first, in Section II, the SRM nonlinear modeling is presented. In Section III the concepts of Port Controlled Hamiltonian System and the theory of PCH modeling of SRM are described. In Section IV a passivity-based robust adaptive controller is designed based on combination of passivity-based current control (PBC) and robust adaptive technique. In Section V, simulation results obtained confirm that the torque ripple reduced in spite of external load disturbances. Finally, conclusions are given in Section VI.

II. Nonlinear Construction and Modeling of SRM

A. SRM Configuration and Basic Principle Operation

The switched reluctance motor has a simple design with a

rotor without windings and stator with windings located at the poles [8]. The principle of operation is based on the tendency of an electromagnetic system to obtain a stable equilibrium position minimizing magnetic reluctance. Whenever diametrically opposite stator poles are excited, the closest rotor poles are attracted, resulting in torque production.

B. Nonlinear Mathematical Model of SRM

An important step in any control system design is to develop a good mathematical model, which represents the plant under various operating conditions. The basic sets of differential equations used to dynamic modeling of the SRM are as follows. First, the electrical state equations of the SRM can be expressed as [1]:

$$v_{\mathrm{k}} = R_{\mathrm{k}} i_{\mathrm{k}} + \frac{\partial \lambda_{\mathrm{k}}(\theta, i_{\mathrm{k}})}{\partial i} \frac{di_{\mathrm{k}}}{dt} + \frac{\partial \lambda_{\mathrm{k}}(\theta, i_{\mathrm{k}})}{\partial \theta} \frac{d\theta}{dt} \tag{1}$$

Where u_k is the phase voltage, i_{k} is the phase current, r_{k} is the phase resistance, $k = a,b,c,d$ is the active phase and $\lambda_{\mathrm{k}}(\theta, i_k)$ is the flux linkage. The flux linkage in an active phase is given by product of self inductance and the instantaneous phase current as:

$$\lambda_{\mathrm{k}}(\theta, i_k) = L_{\mathrm{k}}(\theta, i_k) \cdot i_k \tag{2}$$

While the simplified model for SRM is obtained by substitution of (2) into (1), which results in:

$$L_{\mathrm{k}}(\theta, i_k) \frac{di_{\mathrm{k}}}{dt} = v_{\mathrm{k}} - r_{\mathrm{k}} i_{\mathrm{k}} - \frac{dL_{\mathrm{k}}(\theta, i_k)}{d\theta} i_{\mathrm{k}} \cdot \omega \tag{3}$$

Second, the mechanical state equation of the SRM can be expressed as follows:

$$\frac{d\omega}{dt} = \frac{1}{j}\left\{\sum_{k=a}^{d} T_e(\theta, i_{\mathrm{k}}) - T_{\mathrm{L}} - B\omega\right\} \tag{4}$$

Where j and B are the moment of inertia and viscous friction coefficient, respectively and T_{L} is the load torque. Also, the instantaneous torque $T_e(\theta, i_{\mathrm{k}})$ can be written as:

$$T_{\mathrm{e}}(\theta, i_{\mathrm{k}}) = \frac{1}{2} {i_k}^2 \frac{dL_k(\theta, i_{\mathrm{k}})}{d\theta} \tag{5}$$

III. PCH Modeling of SRM

Energy conserving dynamical systems with independent storage elements can be described by the form of port controlled Hamiltonian (PCH) systems as follows [9]:

$$\begin{cases} \dot{X} = [J(X) - R(X)] \dfrac{\partial H(X)}{\partial X} + g(X)u \\ y = h(X) = g^T(X) \dfrac{\partial H(X)}{\partial X} \end{cases} \tag{6}$$

Where $g(X)$ denotes the input matrix, u and y denote the system input and output. The interconnection structure is captured in the matrix $J(X)$ with $J^T(X) = -J(X)$. The dissipation effects are captured by the matrix $R(X)$ which is a semi-positive definite or positive definite matrix. The total energy of the system is defined by the positive definite function $H(X)$. The port controlled Hamiltonian systems with dissipation (6) satisfy the following power-balance equation:

$$\frac{dH(X)}{dt} = u^T y - \frac{\partial^T H(X)}{\partial X} R(X) \frac{\partial H(X)}{\partial X} \tag{7}$$

The port-controlled Hamiltonian system is passive if the Hamiltonian $H(X)$ is bounded from below [10]. To simplify controller design, a complex system can be decomposed into subsystems by using some techniques of order reduction, such as multi-time-scale analysis. Consider two subsystems in the form of (7) with negative feedback interconnection by the power port p as shown in Fig. 1 [11]. After the interconnection, the closed-loop represented as:

$$\begin{bmatrix} \dot{x}_1 \\ \dot{x}_2 \end{bmatrix} = \left\{ \begin{bmatrix} J_1 - R_1 & 0 \\ 0 & J_2 - R_2 \end{bmatrix} \right\} \begin{bmatrix} \dfrac{\partial H_1}{\partial x_1} \\ \dfrac{\partial H_2}{\partial x_2} \end{bmatrix} + \begin{bmatrix} g_1(u_1 - p y_2) \\ g_2(u_2 + p^T y_1) \end{bmatrix} \tag{8}$$

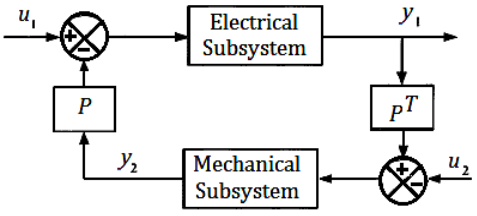

Fig. 1 Negative feedback interconnection of subsystems

For the closed-loop model, the energy function is the total energy of the two subsystems; $H(X) = H_1(X_1) + H_2(X_2)$ therefore, Using (7) and suppose that ${y_1}^T p y_2 = y_2 p^T y_1$, the derivative of this energy function along time is given by:

$$\frac{dH}{dt} = -\frac{\partial^T H_1}{\partial X_1} R_1 \frac{\partial H_1}{\partial X_1} - \frac{\partial^T H_2}{\partial X_2} R_2 \frac{\partial H_2}{\partial X_2} + u_1^T y_1 + u_2^T y_2 \quad (9)$$

Therefore, the stability of the overall closed-loop system can be guaranteed suppose both of the two subsystems are stable.

In [7] it is prove that the complete model of a SRM can be decomposed as the feedback interconnection of the following two passive linked subsystems (electrical and mechanical passive subsystem):

$$\begin{aligned} &\textit{electrical subsystem}: && \begin{bmatrix} v_k \\ -\dot{\theta} \end{bmatrix} \mapsto \begin{bmatrix} i_k \\ T_e \end{bmatrix} \\ &\textit{mechanical subsystem}: && (T_L - T_e) \mapsto -\dot{\theta} \end{aligned} \quad (10)$$

For the interconnected system, using (1), (6) and Take $X_1 = [x_1 \quad x_2 \quad x_3 \quad x_4]^T = [i_a \quad i_b \quad i_c \quad i_d]^T$ as the state vector, the electrical subsystem can be represented as:

$$\begin{cases} D_1 \dot{X}_1 = [J_1(x) - R_1] X_1 + g_1 \left(v_j - p g_2^T X_2 \right) + \xi_1 \\ i_k = g_1{}^T X_1 \end{cases} \quad (11)$$

Where:

$$D_1 = diag(L_a, L_b, L_c, L_d),$$
$$R_1 = diag(R_a, R_b, R_c, R_d) \quad g_1 = diag(1,1,1,1),$$
$$u_1{}^T = [u_a \quad u_b \quad u_c \quad u_d]$$
$$J_1 = 0, \quad \xi_1{}^T = \left[-\frac{1}{2} \frac{dL_k}{d\theta} i_k \omega \right], \quad p = diag\left(\frac{1}{2} \frac{dL_k}{d\theta} i_k \right)$$

Here g_1 denotes the input matrix, u_1 the control vector and ξ_1 the disturbance. Take $X_2 = \omega$ as the state variable for mechanical subsystem, the dynamic property described as:

$$\begin{cases} D_2 \dot{X}_2 = [J_2(x) - R_2] X_2 + g_2 p^T g_1{}^T X_1 + \xi_2 \\ \omega = g_2{}^T X_2 \end{cases} \quad (12)$$

Substituting $D_2 = j$, $R_2 = B$, $g_2 = [1 \quad 1 \quad 1 \quad 1]$, $p = diag\left(\frac{1}{2} \frac{dL_k}{d\theta} i_k \right)$, $\xi_2 = -T_L$ and $J_2 = 0$ (12) can be written as (4).

IV. Passivity-Based Robust Adaptive Control

In this section, we present a PBRAC method for designing SRM controller. The PBRAC block diagram, shown in Fig. 3, is separated into the inner loop and the outer loop controller. Based on the assumption that stator current i_k as well as rotor speed ω are available for measurement, the controller design procedures can be divided into three steps. The first step is Passivity-based current control of the electrical subsystem by injecting a nonlinear electrical damping term. Then a set of reference current vectors $i_k{}^*$ are found out to achieve current tracking. The second step is aimed at reference current generation. The final step is to design a speed controller for speed tracking of the overall system. The sake of the outer loop is to generate the appropriate Torque command fed for the inner loop. Finally, passivity-based inner loop current controller will produce the switching functions.

A. Passivity-Based Inner Loop Control Design

Passivity-based control aimed at achieving the signal regulation is obtained by controlling the suitable energy of the closed-loop system, and add the required damping. The dynamic model (11) can be rewritten as:

$$D_1 \dot{X}_1 + R_1 X_1 = \left(v_j - p g_2^T X_2 \right) + \xi_1 \quad (13)$$

The objective of PBC design is to guarantee tracking of signal i_k toward to its desired state i_k^* [12]. This method proposes to make a copy of (15), where the state X_1 is replaced by the desired state X_1^* and the injection damping term is added, that is a desired system:

$$D_1 \dot{X}_1^* + R_1 X_1^* - K\tilde{X}_1 = \left(v_j - p g_2^T X_2^* \right) + \xi_1 \quad (14)$$

Where the injection damping term is $K = diag\{k_1, k_2, k_3, k_4\}$, referred as damping injection matrix, is a positive definite diagonal matrix and $\tilde{X}_1 = X_1 - X_1^*$. Subtracting (14) from (13) yields the following error dynamic model:

$$D_1 \dot{\tilde{X}}_1 + R_1 \tilde{X}_1 + K\tilde{X}_1 + p g_2^T \tilde{X}_2 = 0 \quad (15)$$

Thus, we can define desired storage energy function $H_d = 0.5 \tilde{X}_1^T D_1 \tilde{X}_1$ as a Lyapunov function. The desired equilibrium point is realized if the Hamiltonian H has its minimum at the equilibrium point. Asymptotic stability is proved using LaSalle's invariance principle for the closed-loop system (15) where:

$$\frac{d}{dt} H_d = -\tilde{X}_1{}^T (R_1 + K) \tilde{X}_1 \quad (16)$$

Following LaSalle's theorem, the time derivative of storage energy function is forced to be negative semidefinite, i.e. $\dot{H}_d \le 0$, being equal to zero only for the equilibrium

points. Therefore (16) is equal to zero only when $\tilde{X}_1 = 0$. The Lyapunov stability and convergence can be proven that (13) is passive and input-output stable. Finally, the above method proceeds to restrict $X_1 = X_1^*$ and solve from (14), which yields the switching functions as:

$$v_k = R_k i_k^* + L_k \frac{di_k^*}{dt} + \frac{1}{2}\frac{\partial L_k}{\partial \theta} i_k \omega + \frac{1}{2}\frac{\partial L_k}{\partial \theta} i_k \omega^* - K\left(i_k - i_k^*\right) \tag{17}$$

The reference current is calculated by using the desired torque:

$$i_k^* = \sqrt{\frac{2T_e^*}{dL_k(\theta, i_k)/d\theta}} \tag{18}$$

Where $dL_k(\theta, i_k)/d\theta$ is obtained by using the look-up table that shown in Fig 2.

A. Robust Adaptive Outer Loop Speed Controller

After inner-loop controller generates suitable reference current, the final step is to design the outer-loop speed controller to determine the appropriate reference torque. For speed control design purposes, the dynamic model of the SRM can be written as:

$$\frac{d\omega}{dt} = \frac{1}{j}\{T_e - T_L - B\omega\} = \beta$$
$$\frac{d\alpha}{dt} = \frac{1}{J}\left\{\sum_{k=a}^{d}\left(\frac{\partial T_e}{\partial i_k}\right)\left(\frac{\partial \lambda_k}{\partial i_k}\right)^{-1}\left(v_k - R_k i_k - \frac{\partial \lambda_k}{\partial \theta}\omega\right)\right\} + \frac{1}{J}\left\{\omega\sum_{k=a}^{d}\left(\frac{\partial T_e}{\partial \theta}\right) - T_u - B\alpha\right\} \tag{19}$$

Where $T_u = \dot{T}_L$, Let $x = (x_1 \quad x_2)^T = (\beta \quad \omega)^T$, Also let the output of the SRM be $y = \omega$. Thus, the model of the SRM system can be written in compact form as $\dot{y} = f(x) + g(x)u$, where f and g are determined from (19). We consider $T_u(t) \in \Omega_\alpha = \{T_u(t) : |T_u(t)| \le \alpha\}$ as an external disturbance and control law as:

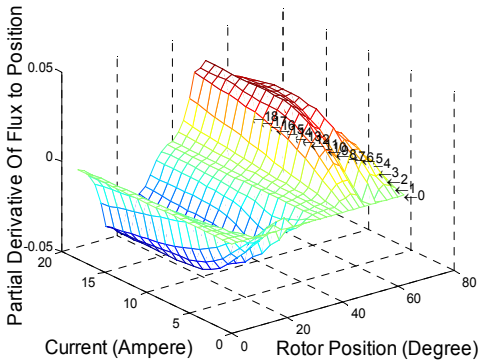

Fig. 2 Partial derivative of flux to position

$$u = \frac{-1}{g}\left[Ke + \frac{\left(f - \dot{\omega}^*\right)^2 e}{\left|(f - \dot{\omega}^*)e\right| + \delta_1 \exp(-\sigma_1 t)}\right] + \frac{-1}{g}\left[\hat{\alpha}^2 \frac{e}{\left|e\right|\hat{\alpha} + (\delta_2 / p)\exp(-\sigma_2 t)}\right] \tag{20}$$

Where $K > 0$, is the state feedback gain and $\hat{\alpha}$ denotes the estimated value of the unknown parameter α. The constants δ_i and σ_i $i = 1,2$ are (small) positive constants specified by the designer to avoid discontinuity and control chattering. The control law (20) with adaptation mechanism $\dot{\hat{\alpha}} = \gamma|e|$, where $\gamma > 0$ is adaptation gain, guarantees that all the closed loop signals are bounded and tracking error $e = \omega - \omega^*$ is asymptotically converged to zero. Clearly, the smaller value of δ_i, give less smoothness to the control law [13], [14].

V. Simulation Results

The SRM system is simulated using the MATLAB software. The model takes magnetic saturation into account. The parameters of the motor used for the simulation studies are given in Table 1.

The motor is commanded to accelerate from rest to 200 RPM under a sudden load change from 3 Nm to 6 Nm. Fig. 4 shows speed response when corresponding to robust adaptive speed control law described by (21) and the proposed PBRAC algorithm for the precise plant model. It can be seen that there is a steady error on the response of robust adaptive speed control without using of PBC, whereas there is no steady error for the proposed algorithm. Also, transient response of the proposed PBRAC due to an external disturbance quickly damped. Hence, there is a considerable improvement of the steady state and transient responses.

The proposed controller is applied to implement the torque ripple minimization. The torque ripple is defined as [15]:

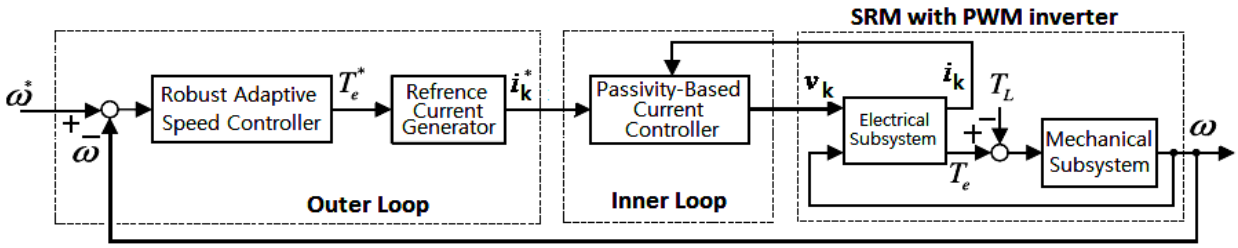

Fig. 3 Block diagram of the overall speed control system

$$Torque\ Ripple = \frac{T_{inst}(\max) - T_{inst}(\min)}{T_{avg}} \quad (21)$$

Torque profiles of the conventional robust adaptive and proposed PBRAC are being displayed in Fig. 5. There are significant amount of torque ripples when only the conventional robust adaptive is used. But, the instantaneous torque of the proposed PBRAC is highly improved with much lower torque ripples.

As can be seen from Table 2, when the load torque is 3 Nm, the percentage peak-to-peak torque ripple of robust adaptive passivity-based control reduces 2.94% compared with that of the robust adaptive control. When the load torque is 6 Nm, the torque ripple factor reduces 0.3%.

TABLE I
PARAMETERS OF THE SRM

Parameters	Rating values
Output Power	*4 KW*
Rated Speed	*1500 RPM*
Number of Stator Poles	*8*
Inertia(J)	*0.008 N .ms* ^{2}
Damping Factor(B)	*0.00078 N .ms*
Phase Resistance	*0.75* Ω
Dc Voltage Supply	*280 V*

TABLE II
TORQUE RIPPLE PERCENTAGE

Control strategy	Load Torque	
	3 Nm	6 Nm
Conventional Robust Adaptive	6.7 %	1.8%
RAPBC	3.76 %	1.5%

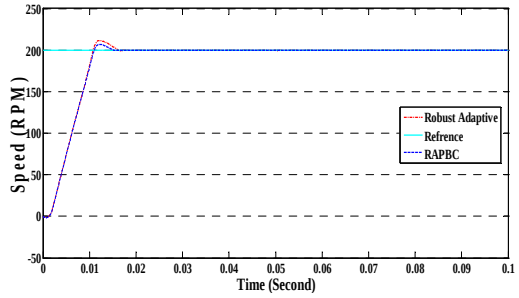

(a)

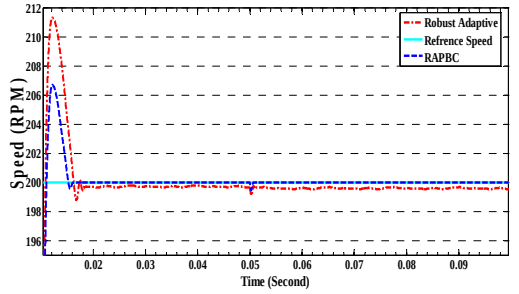

(b)

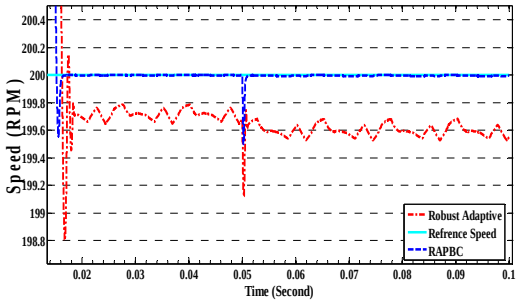

(c)

Fig. 4 (a) The speed profile upon the variation of load torque at t=0.05 s. (b) and (c) are zoom of (a)

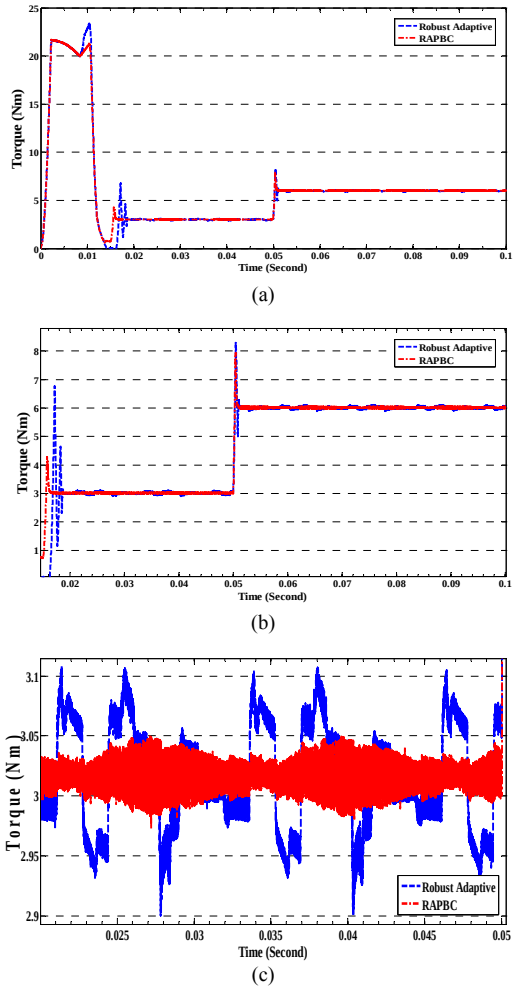

Fig. 5 (a) The SRM produced torque profile. (b) and (c) are zoom of (a)

VI. Conclusion

In this paper, a robust adaptive PBC algorithm is proposed for torque ripple reduction and precise speed tracking. By decomposing the SRM driving system into an electrical subsystem and a mechanical subsystem, the order of the system is reduced. The passivity-based controller is designed for the electrical subsystem based on the two-time-scale and passivity properties. Because of the strict passivity of the two subsystems and their negative feedback interconnection, stability of the proposed controller for the whole driving system can be achieved. The results demonstrate that the proposed robust adaptive PBC for SRM possesses excellent performance and torque ripple minimization compared with conventional robust adaptive control.

References

[1] R. Krishnan, Switched Reluctance Motor Drives, Boca Raton, FL:CRC Press, 2001.

[2] T. S. Chuang, and C. Pollock, "Robust speed control of a switched reluctance vector drive using variable structure approach," *IEEE Trans. on Industrial Electronics*, vol. 44, no. 6, pp. 800–808, Dec. 1997.

[3] A. D. Cheok, and Z. Wang, "Fuzzy Logic Rotor Position Estimation Based Switched Reluctance Motor DSP Drive With Accuracy Enhancement," *IEEE Trans. on Power Electronics*, vol. 20, no. 4, pp. 908-921, July 2005.

[4] S. K. Panda and P. K. Dash, "Application of nonlinear control to switched reluctance motors: A feedback linearization approach," *IEE Proc.-Electric Power App.s*, vo1. 43, no. 5, pp. 371–379, Sept. 1996.

[5] B. Ge, X. Wang, P. Su, and J. Jiang, "Nonlinear internal-model control for switched reluctance drives," *IEEE Trans. on Power Electronics*, vol. 17, no. 3, pp. 379–388, May 2002.

[6] R. Ortega, A. van der Schaft, I. Mareels, and B. Maschke, "Putting energy back in control," *IEEE Contr. Syst. Mag.*, vol. 21, no. 2, pp. 18–33, Apr. 2001.

[7] G. Espinosa-Pe´rez, P. Maya-Ortiz, M. Velasco-Villa, and H. Sira-Ramírez, "Passivity-based control of switched reluctance motors with nonlinear magnetic circuits," *IEEE Trans. On Control System Technology*, Vol. 12, no. 3, pp 439–448, May 2004.

[8] V. Ramanarayanan and D.Panda, "Mutual Coupling and Its Effect on Steady-State Performance and Position Estimation of Even and Odd Number Phase Switched Reluctance Motor Drive," *IEEE Trans. On Magnetics*, vol. 43, no. 8, pp. 3445–3456, August 2007.

[9] S. Stramigioli and H. Bruyninckx, Geometric Network Modeling and Control of Complex Physical Systems. Berlin, Germany: Springer-Verlag, 2008.

[10] R. Ortega, A. van der Schaft, B. Maschke, and G. Escobar, "Interconnection and damping assignment passivity-based control of port-controlled hamiltonian systems," *Automatica*, vol. 38, no. 4, pp. 585–596, 2002.

[11] J.E. Slotine and W. Li, Applied Nonlinaer Control, Prentice Hall, 2002.

[12] R. Ortega, A. Loria, P. J. Nicklasson, and H. Sira-Ramirez, Passivity-based Control of Euler-Lagrange Systems. Mechanical Electrical and Electromechanical Applications: Springer-Verlag, 1998.

[13] M. M. Namazi, S. M. Saghaiannejad, and A. Rashidi, "Robust Adaptive Speed control of Switched Reluctance Motor Considering Torque Ripple Minimization, " 18th Annual Conf. Electric. Eng. Iran, pp. 1787-1792, May 2010.

[14] H.R. Koofigar, S. Hosseinnia, and F. Sheikholeslam, "Robust adaptive nonlinear control for uncertain control-affine systems and its applications," *Nonlinear Dynamics*, Springer Science Publishing, vol. 56, no. 1, pp. 13-22, June 2008.

[15] Iqbal Husain, "Minimization of Torque ripple in SRM drives," *IEEE Trans. on Industrial Electronics*, vol. 49, no. 1, pp. 28-39, Feb. 2002.